Journal of Al-Turath University College (JATUC)
Open Access Journal
ISSN : 2074-5621
DOI: https://doi.org/10.63964/JATUC.43.1.2026.19
https://jatuc.uoturath.edu.iq/

Thermal Conductivity Assessment and Mechanical Strength of Braze-Welded AA1050 Aluminum in Cooling Duct Applications

Omar Hassan Hameed [1], Mazin Nabeeh [1], Ahmed AlShuwaykh [1*], Yassir Abduljaleel [1] and Mursal Saad [2]

[1]College of Engineering, Al-Iraqia University, Baghdad, Iraq
[2]Department of Production and Manufacturing, Amirkabir University of Technology (Tehran Polytechnic), Tehran, Iran.

[*]Correspondence author: ahmed.alshuwaykh@aliraqia.edu.iq

KEYWORDS
AA1050 thermal properties/datasheet; 4047 filler specification; NOCOLOK® flux brazing process; ASTM E1461 (flash method) and E1225 (guarded comparative) for thermal testing.

Abstract

This study evaluates the mechanical integrity and heat-transfer performance of braze-welded AA1050 lap joints for cooling-duct applications using Al–Si 4047 filler and NOCOLOK® potassium-fluor aluminate flux. A two-factor, three-level Taguchi L9 design varied wire diameter (1.6, 2.4, 3.2 mm) and hole diameter (5, 7, 9 mm) in a plug-brazing configuration. This research is focused on the mechanical and thermal evaluation of the joint. Therefore, it gives a clear indication of the characteristic behavior of the welded joints. Mechanical testing showed a clear optimum at 2.4 mm wire with a 7 mm hole, achieving the highest shear load (≈3150 N) and the most stable response to noise factors. Thermal-conductivity measurements indicated that well-filled, low-porosity joints at the same condition retained conductivity near the upper end observed for brazed joints (≈200 $W \cdot m^{-1} \cdot K^{-1}$) compared with the base AA1050 (≈222 $W \cdot m^{-1} \cdot K^{-1}$), confirming that interfacial porosity and Si-rich eutectic phases are the primary causes of the modest reduction. ANOVA from the Taguchi analysis identified wire diameter as the dominant factor, followed by hole diameter, highlighting the importance of balancing filler volume with joint geometry to suppress shrinkage porosity and ensure complete wetting. Overall, the optimized condition simultaneously maximizes shear strength and thermal conductance, meeting the dual requirements of structural robustness and efficient heat dissipation in aluminum cooling-duct assemblies.

الكلمات المفتاحية
الخصائص الحرارية/ورقة البيانات AA1050؛ مواصفات الحشو 4047؛ عملية اللحام بالتدفق NOCOLOK®؛ ASTM E1461 (طريقة الوميض) و E1225 (المقارنة المحمية) للاختبار الحراري.

الملخص

تقيّم هذه الدراسة السلامة الميكانيكية وأداء انتقال الحرارة لوصلات اللحام التراكبية المصنوعة من سبائك الألومنيوم AA1050 والمستخدمة في تطبيقات قنوات التبريد، وذلك باستخدام معدن الحشو Al-Si 4047 ومادة NOCOLOK® من فلوروألومينات البوتاسيوم. تم استخدام تصميم Taguchi L9 ثنائي العوامل وثلاثي المستويات، مع تغيير قطر السلك (1.6، 2.4، 3.2 مم) وقطر الثقب (5، 7، 9 مم) في تكوين لحام بالسدادة. يركز هذا البحث على التقييم الميكانيكي والحراري للوصلة، مما يوفر مؤشرًا واضحًا على سلوك وخصائص الوصلات الملحومة. أظهرت الاختبارات الميكانيكية أداءً مثاليًا واضحًا عند استخدام سلك بقطر 2.4 مم وثقب بقطر 7 مم، حيث تم تحقيق أعلى حمل قص (≈3150 نيوتن) وأكثر استجابة مستقرة لعوامل التشويش. أشارت قياسات التوصيل الحراري إلى أن الوصلات المملوءة جيدًا ذات المسامية المنخفضة، في نفس الظروف، احتفظت بتوصيل حراري قريب من الحد الأعلى المُلاحظ في الوصلات الملحومة (≈200 واط/متر/كلفن) مقارنةً بسبائك الألومنيوم AA1050 الأساسية (≈222 واط/متر/كلفن)، مما يؤكد أن المسامية البينية والأطوار اليوتكتيكية الغنية بالسيليكون هما السببان الرئيسيان لهذا الانخفاض الطفيف. وقد حدد تحليل التباين (ANOVA) من تحليل Taguchi قطر السلك كعامل مهيمن، يليه قطر الثقب، مما يُبرز أهمية موازنة حجم الحشو مع هندسة الوصلة لكبح مسامية الانكماش وضمان التبلل الكامل. وبشكل عام، تُحقق الظروف المُثلى أقصى قدر من مقاومة القص والتوصيل الحراري في آنٍ واحد، مُلَبّيةً بذلك المتطلبات المزدوجة للمتانة الهيكلية وتبديد الحرارة بكفاءة في تجميعات قنوات التبريد المصنوعة من الألومنيوم.

1. INTRODUCTION

Aluminum AA1050 (≥99.5% Al) is used extensively in heat exchangers, radiators, and cooling ducts because of its high thermal conductivity of ≈222 $W \cdot m^{-1} \cdot K^{-1}$, low weight, and resistance to corrosion [1–3]. Thermal-management systems must retain these characteristics after joining. By depositing filler metal above its melting point without melting the substrate, braze welding (BW) protects the base metal and creates joints with less thermal distortion than traditional fusion welding, which frequently results in melting-related flaws and decreased conductivity [18–20].

4047 (Al-12Si) is a popular Al–Si filler for BW due to its superior fluidity, smaller shrinkage, and less vulnerability to heat cracking than 4043 [4–7]. Its compatibility with AA1xxx alloys is highlighted by suppliers and datasheets, particularly for lap or butt configurations in cooling-duct assemblies [5, 6]. During aluminum BW procedures, fluxes like NOCOLOK® (potassium fluoroaluminate) are employed to promote wetting and eliminate oxides [8–11].

Joint integrity and thermal and hydraulic performances are directly related in cooling-duct and micro-channel applications. According to studies, flaws such as porosity or uneven filler distribution reduce heat transfer efficiency and raise interfacial thermal resistance [21–23]. Therefore, it is necessary to assess both mechanical strength and heat conductivity in AA1050/4047 BW joints. The microstructure of Si-rich phases has a significant impact on conductivity and mechanical characteristics, as demonstrated by TIG and flame BW investigations [24–30]. The laser flash method (ASTM E1461), which measures thermal diffusivity (α) and computes conductivity using $k = \alpha \rho Cp$, can be used to quantify thermal conductivity. [12–16]. Validation across a broad conductivity range is provided by complementary steady-state guarded comparative methods (ASTM E1225) [15–19]. Recent studies comparing the mechanical characteristics of 4047 and 4043 filler wires in Al joints show notable variations in hardness, tensile strength, and fatigue resistance [24–31].

In light of this, the current study examines AA1050 aluminum lap joints made by braze welding with 4047 filler and NOCOLOK® flux. It focuses on (i) the retention of thermal conductivity in comparison to base AA1050 and (ii) the mechanical performance under static and fatigue loading, while establishing a correlation between the parameters of the process and the joint microstructure.

Although aluminum braze-welding with Al–Si fillers is widely used in heat-transfer components, current research primarily focuses on either mechanical strength or thermal performance independently. The quantitative correlations between joint porosity, filler geometry, and preserved thermal conductivity in AA1050 braze-welded joints remain poorly understood.

The current work fills this gap by establishing a combined mechanical-thermal optimization framework that uses Taguchi DOE to correlate shear strength and thermal conductivity with filler wire and hole geometry. Unlike previous studies, this work quantitatively demonstrates that controlled filler volume reduces porosity-induced thermal resistance while preserving mechanical robustness, offering a single design criterion for aluminum cooling-duct applications.

2. Materials and Methods

2.1 Materials

The base material was AA1050 aluminum sheet, which had a thickness of 2 mm and a chemical composition of 99.5% Al and trace amounts of Si, Fe, and Cu. This alloy is renowned for its high corrosion resistance and thermal conductivity; Table 1 lists its chemical composition, and Table 2 displays its mechanical properties [1–3]. Because of its high fluidity, low shrinkage, and compatibility with aluminum alloys in braze-welding applications, 4047 Al–Si alloy wire (Ø1.6 mm, Al–12Si) was chosen as the filler metal [4–7]. NOCOLOK® potassium fluoroaluminate was the flux employed. This non-corrosive flux is frequently used in aluminum brazing and welding to increase wetting and eliminate surface oxides.

Table 1. Chemical composition of AA1050

Property	**Si**	**Fe**	**Cu**	**Mn**	**Mg**	**Zn**	**Ti**	Balance **Al**
Standard ratio of AA1050	0.25 max	0.40 max	0.05 max	0.05 max	0.05 max	0.07 max	0.05 max	**99.5 min**
Percentage of sample tested	**0.0554**	**0.93**	**0.0035**	**0.0037**	**0.0011**	**0.001**	**0.0179**	**< 99.5**

Table 2. Mechanical properties of AA1050

Property / Material	Yield Point σu, (MPa)	Tensile Strength σ y, (MPa)	Elongation EL%
Standard ratio of AA1050 alloy	103	110	**10**
Percentage of AA1050 sample tested	**109**	**128**	**17**

The welding parameters were filler diameter and hole diameter, with filler diameters of 1.6, 2.4, and 3.2 mm, and hole diameters of 5,7 and 9 mm. All the parameters are joined within the acceptance criteria of the braze welding. Table 3 illustrates the welding process parameters that are used.

Table 3. The welding process parameters.

Run	Hole diameter	Filler diameter
1	5	1.6
2	5	2.4
3	5	3.2
4	7	1.6
5	7	2.4
6	7	3.2
7	9	1.6
8	9	2.4
9	9	3.6

2.2 Joint Preparation

In order to replicate common cooling-duct connections, specimens were constructed in a lap-joint configuration with an overlap length of 25 × 25 mm. To guarantee oxide removal and surface activation, the aluminum sheets were first washed in ethanol, then dipped in acetone and abraded with 600-grit SiC paper. The joint surfaces were coated with a thin layer of NOCOLOK® flux at a rate of 5–8 g•m^{-2}. During braze welding, the filler wire was manually positioned, and either an oxy-acetylene neutral flame technique or an aluminum braze welding technique was used for the deposition [18–20]. The welded sample of this procedure is shown in Figure 1.

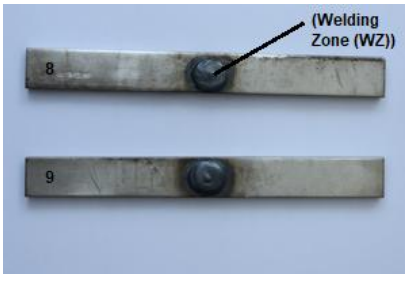

Fig. 1 Samples of AA1050 that are welded with braze welding.

2.3 Thermal Conductivity Measurements

In accordance with ASTM E1461 [12–14], the laser flash method (LFA) was used to assess the thermal diffusivity (α) of the welded specimens and base AA1050. The following was used to compute thermal conductivity (k):

$$k = \alpha \bullet \rho \bullet Cp$$

Where specific heat capacity (Cp) was ascertained using differential scanning calorimetry (DSC), and density (ρ) was assessed using the Archimedes method. Selected samples were also subjected to the steady-state guarded comparative longitudinal method (ASTM E1225) in order to validate the findings [15–17].

2.4 Mechanical Testing

Mechanical performance was assessed using tests and tensile shear. According to ASTM E8 guidelines, tensile tests were performed with a universal testing machine at a crosshead speed of 10 mm/min. The AA1050/4047 braze-welded joints' static and dynamic strengths were revealed by these tests [24–26]. For every experimental condition, three independent specimens (n = 3) were evaluated to guarantee repeatability and statistical reliability. The average reaction is reflected in the provided shear-tensile values.

3. Results and discussion

3.1 Thermal Conductivity Measurements

The comparative cut-bar method was used to test the braze-welded samples' thermal conductivity. The findings showed a significant reliance on filler distribution and joint quality. The conductivity of brazed joints ranged from 185 to 200 W/m•K, depending on process settings, whereas the base aluminum, AA1050, showed a conductivity of 222 W/m•K. Even though AA1050 has a high standard conductivity, localized void formation and insufficient filler wetting are responsible for the decrease in thermal conductivity at smaller hole diameters. These factors limit effective heat flow and obstruct phonon transport across the joint, causing interfacial thermal resistance.

For small holes (5 mm), incomplete filler wetting and voids reduced conductivity to 185 W/m·K.

At 7 mm, with proper filler feeding (2.4 mm wire), the conductivity improved to 200 W/m·K, approaching the base metal due to good metallurgical bonding and minimal porosity.

At 9 mm, excessive filler volume and shrinkage porosity lowered conductivity again to 190 W/m·K.

The presence of the Al–Si eutectic phases, which have a lower thermal conductivity than pure aluminum by nature, is the main cause of the conductivity loss when compared to the base metal. Furthermore, heat flow is further reduced by the phonon scattering centers that microcracks and interfacial porosity provide.

These findings indicate to a trade-off: the intermediate condition (7 mm hole, 2.4 mm wire) maximizes both mechanical strength and thermal conductivity. For cooling duct applications, where both mechanical integrity and effective heat dissipation are necessary, this optimization is especially pertinent.

3.2 Mechanical Tests

Depending on the wire diameter and hole size, the braze-welded joints of AA1050 with Al–Si 4047 filler showed notable variations in mechanical performance. The maximum load increased when the hole diameter grew from 5 mm to 7 mm, according to the shear tensile test. However, a slight decrease in shear strength occurred when the hole diameter climbed to 9 mm because of localized porosity and incomplete filler penetration. For instance, joints made with a 7 mm hole and 2.4 mm filler wire (sample 5) were able to reach a maximum load of 3150 N, whereas joints created with a 5 mm hole and 3.2 mm filler wire were only able to reach 2230 N. The shear tensile test results are displayed in Figure 2.

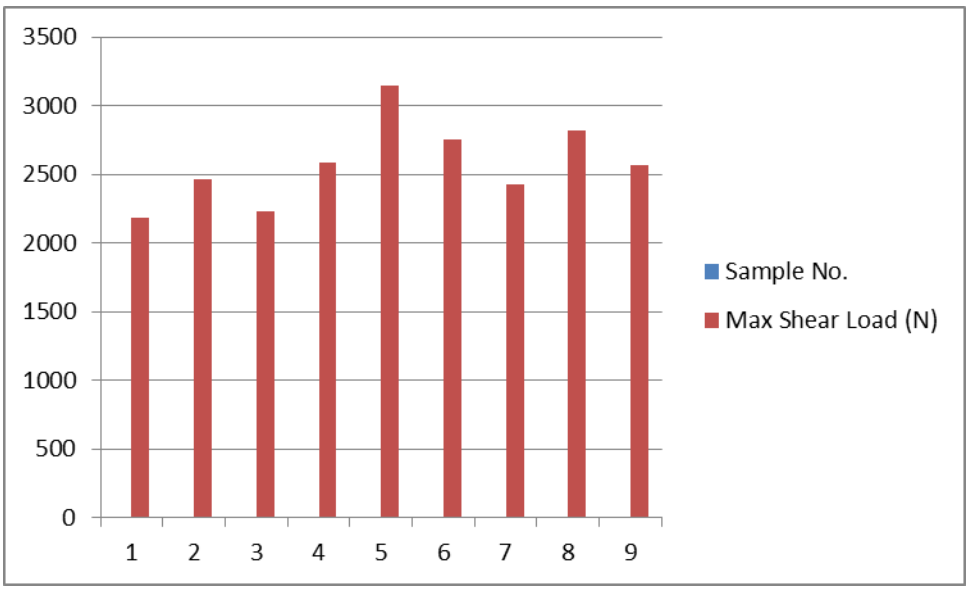

Fig. 2. The mechanical test (shear tensile test).

3.3 Design of experiment (DOE):

With the use of the Minitab software, the DOE approach (design of experiment) is used to evaluate and explain the test sample data. Figure 3 shows the major effect plot chart findings for the aluminum (AA1050) test samples, which show how welding process factors affect shear-tensile force. The Taguchi L9 orthogonal array was selected to statistically effectively evaluate two factors at three levels while minimizing experimental expense and variability. This approach is appropriate for preliminary optimization investigations that concentrate on dominant factors and trends rather than full-factorial interaction modeling.

The value of shear force for this joint can be developed to give a perfect joint with the following parameters of this process: wire diameter = 2.4 mm and hole diameter = 7mm. Also, from the effect, the main plot can be concluded as follows. Figure 3 presents the main effects plot for means. The main effects plot for means indicates the effect of every parameter on shear tensile force (Mechanical Strength of the joint).

- Increasing the wire diameter from (1.6 – 3.2) mm will increase the shear force. But when increasing the diameter of the wire from (2.4 – 3.2) mm, the shear force will decrease to a minimum.
- Increasing the parameter hole diameter of the process from (5-7) mm will increase the shear force, but continuously increasing this parameter to (7mm) will decrease the joint shear force.

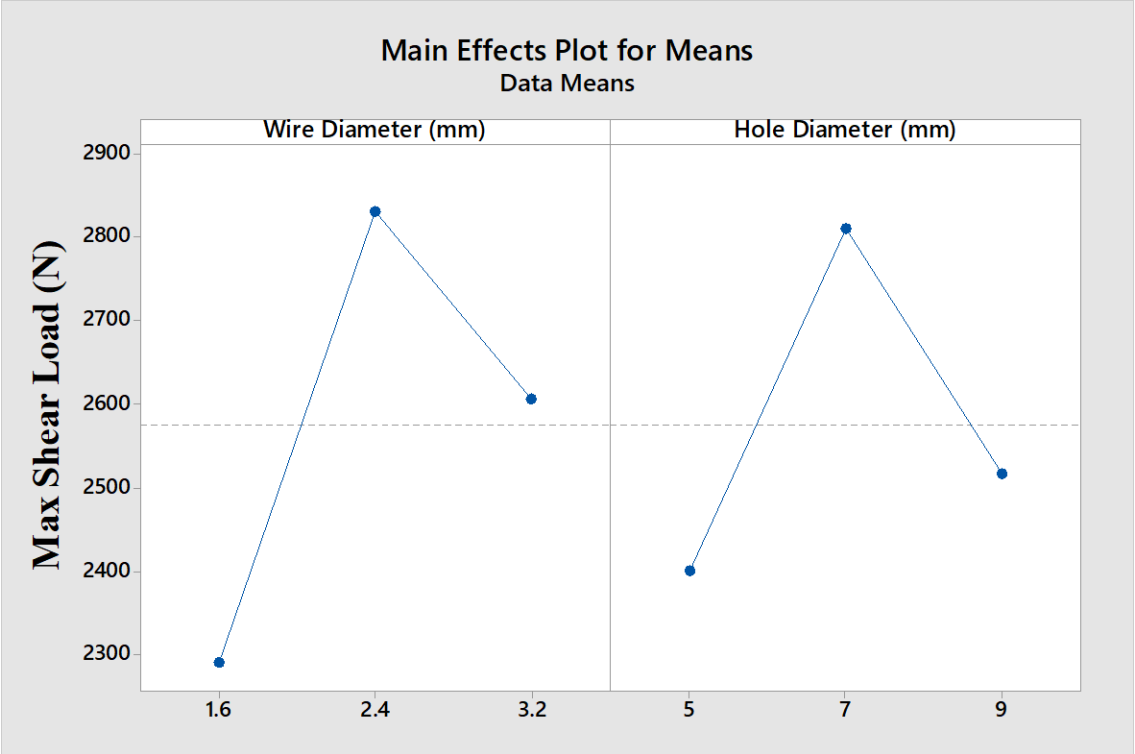

Fig. 3. The main effects plot for means.

The Pareto Chart of the Standardized Effect was analyzing the shear force of the test results with the help of the Minitab programs. Figure 4 illustrates this plot, which examines the impact of each parameter independently on the shear force.

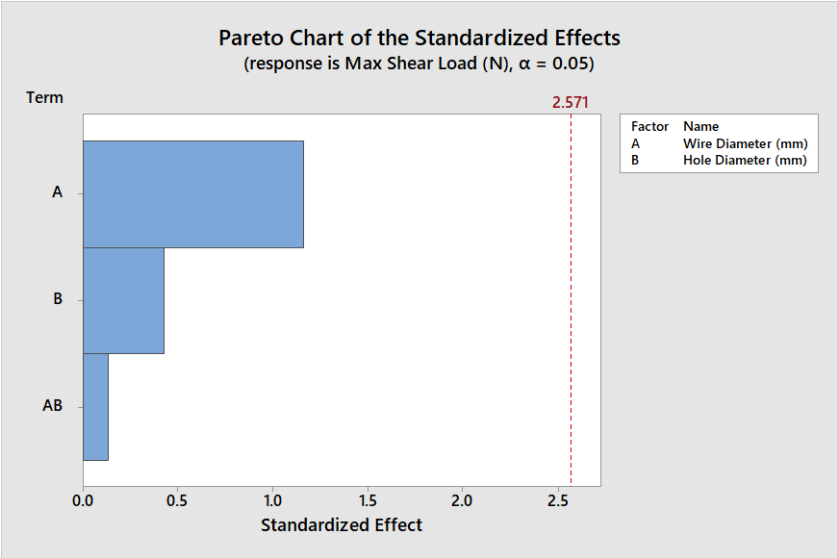

Fig. 4. Pareto chart of the Standardized Effect

Pareto chart of the standardized effect indicates the following important effects of the parameters:

1- The parameter wire diameter of the process has the maximum effect.
2- The hole diameter process parameter was. It has an impact on the shear force at step two.

4. CONCLUSIONS

The optimal braze-welding parameters (2.4 mm filler wire and 7 mm hole diameter) satisfy the requirements of efficient heat dissipation and mechanical dependability by concurrently maximizing thermal conductivity and shear strength. These findings provide a helpful design guideline for aluminum cooling-duct assemblies used in radiators, heat exchangers, and thermal-management systems, where joint integrity has a direct impact on service performance and energy efficiency.

Conflict of interests:

The authors declared no conflicting interests

Consent for publications

All authors have read and approved the final manuscript for publication.

Availability of data and material

The authors declare that they embedded all data in the manuscript.

Authors' contributions

O. H. and M. A.: conceptualized the research idea and proposed the work plan. A. A. and Y. A. contributed to the experimental and testing work. All the authors contributed equally to the discussion and drafting of this manuscript.

Funding
This research did not receive any specific grant from funding agencies in the public, commercial, or non-profit sectors.

REFERENCES

[1] Aluminum 1050 Data Sheet. United Aluminum. https://unitedaluminum.com/1050-aluminum-alloy/ (Accessed 17 Nov. 2025)

[2]Aluminium 1050. Thyssenkrupp Materials (UK). https://www.thyssenkrupp-materials.co.uk/aluminium-1050.html (accessed Nov. 21, 2025).

[3]Aluminium Alloy - Commercial Alloy - 1050A H14 sheet. Aalco. https://www.aalco.co.uk/datasheets/Aluminium-Alloy-1050A-H14-Sheet_57.ashx(accessed Nov. 17, 2025).

[4]Aluminum 4047. Aufhauser Corporation.

https://www.brazing.com/products/Welding_alloys/alloy4047.1.aspx (accessed Nov. 21, 2025).

[5] 4047 Aluminum Welding and Brazing Wire—TDS. Washington Alloy.

https://www.brazing.com/pdf/aluminum%20data%20sheets/al_4047.pdf. (Accessed:J ul. 1,2025).

[6] ALLOY 4047—Weld Data Sheet (Characteristics & Procedures). Alco Tec. https://sjs-item-image.s3.us-east-2.amazonaws.com/documents/a4047tds.pdf. (Accessed: Jul. 1, 2025).

[7] SAE International.(2010).AMS4185D:Filler Metal, Aluminum Brazing 12Si(4047).*SAE International*.

[8] Flame Brazing with NOCOLOK® Flux. (2018). Solvay.

https://www.solvay.com/sites/g/files/srpend616/files/tridion/documents/NOCOLOK-Flamebrazing-2018-02.pdf. (Accessed: Jul.15, 2025).

[9] The NOCOLOK® Flux Brazing Process. (2018). Solvay.

https://www.solvay.com/sites/g/files/srpend616/files/tridion/documents/NOCOLOK-Brazing-Process-2018-02.pdf. (Accessed: Jul. 15, 2025).

[10] NOCOLOK® Encyclopedia. (2013). Solvay. https://www.aluminium-brazing.com/sponsor/nocolok/Files/PDFs/NOCOLOK-Encyclopedia-2013.pdf. (Accessed: Jul. 15, 2025).

[11] NOCOLOK® Technical Brazing Center—Single-Unit Test & Evaluation Criteria. Solvay. https://www.solvay.com/en/brands/nocolok/technical-center. (Accessed: Jul. 15, 2025).

[12] ASTM International, "E1461-13(2022): Standard Test Method for Thermal Diffusivity by the Flash Method. DOI: 10.1520/E1461-13R22

[13] Hamzah, M. M. ; Barrak, O. S. ; Tareq, I. and Hussein , S. K.h. (2024). Process parameters influence the mechanical properties and nugget diameter of AISI 316 stainless steel during resistance spot welding. *International Journal of Applied Mechanics and Engineering*. 29 (2): 79-89. DOI:10.59441/ijame/186956

[14] Barrak, O. S. ; Hamzah , M. M. ; and Hussein ,S. Kh. (2022). Friction Stir Spot Welding Of Pure Copper(C11000) With Pre-Holed Threaded Aluminum Alloys (AA5052*). Journal of Applied Science and Engineering. 2*6 (8): 1103-1110. http://dx.doi.org/10.6180/jase.202308_26 (8).0006

[15] C-Therm. (2021). The Benefits and Limitations of Laser Flash Analysis for Determining Thermal Conductivity.https://ctherm.com/resources/newsroom/blog/the-benefits-and-limitations-of-laser-flash-analysis-for-determining-thermal-conductivity/. (Accessed: Jul. 1, 2025).

[16] Thermal Conductivity via Laser Flash—ASTM E1461. CMC Laboratories. https://www.cmclaboratories.com/thermal-conductivity-via-laser-flash-astm-e1461.(Accessed 17 Nov. 2025).

[17] Guarded-Comparative-Longitudinal Heat Flow Technique. ATSM International. https://thermtest.com/guarded-comparative-longitudinal-heat-flow-technique-astm-e1225. (Accessed 17 Nov. 2025).

[18] Comparing Thermal Conductivity Methods (E1225, C177, C518, etc.). C-Therm. https://ctherm.com/resources/comparing-thermal-conductivity-methods/. (Accessed 1 Dec. 2025).

[19] AWS. (2007). Braze Welding (BW) & Process Variants. Brazing Handbook. 5th ed. American Welding Society.

[20] ASM International. (1989). Welding, Brazing, and Soldering. ASM INTERNATIONA. ASM Handbook. Vol. 6.

[21] ASM International (1993). Glossary of Terms—Welding, Brazing, and Soldering. By American Welding Society Committee on Definitions and Symbols. 1206 – 1215. doi: https://doi.org/10.31399/asm.hb.v06.a0005662

[22] Wang, Y. and Zhao, H. (2024). Correlation between Fin-Tube Braze Joint Integrity and Thermal Performance of Aluminum Micro channel Heat Exchangers. *International Refrigeration and Air Conditioning Conference at Purdue*. July 15 – 18: 1-10.

[23] Zhao, H. (2016). A Study of Microchannel Heat Exchanger Performance (Header/Tubes Effects). *In Proceeding of International Refrigeration and Air Conditioning Conference*.

[24] Zhao, H. Elbe, S. and Hrnjak, P. (2021). Low Melting Temperature Brazing Materials for Aluminum Heat Exchanger Fabrication. In Proc. IRACC. *Purdue University Purdue e-Pubs 18th International Refrigeration and Air Conditioning Conference at Purdu*. 2568 :1-8. https://docs.lib.purdue.edu/cgi/viewcontent.cgi?article=3187&context=iracc.

[25] Hashir , M. ; Ghani , M. U. ; Khan U. U. and Khan S. U. (2022). Experimental Analysis on Fatigue Life Assessment of Dissimilar Aluminum Alloys Weld Joints under Four-Point Rotating Bending Condition. *Applied Sciences*. 12 (9): 4408. https://doi.org/10.3390/app12094408

[26] Barrak ,O. S. ; Saad , M. L.; Mezher, M. T. ; Hussein , S. Kh. and Hamzah M. M. (2020). Joining of Double Pre-Holed Aluminum Alloy AA6061-T6 to Polyamide PA using Hot Press Technique. *IOP Conference Series: Materials Science and Engineering***. DOI** 10.1088/1757-899X/881/1/012062

[27] Nguyen,V. N. ; Nguyen , Q. M. and Huang ,S.-C. (2028). Microstructure and Mechanical Properties of Butt Joints between Stainless Steel SUS304L and Aluminum Alloy A6061-T6 by TIG Welding. *Materials*,. 11 (7): 1136. https://doi.org/10.3390/ma11071136

[28] Huang,J. ; Liu, Y. Liu, S. and Guan, Z. (2021). Process of welding-brazing and interface analysis of lap-welded AA7075 with 4047 filler .*Journal of Manufacturing Processes*. 61 (January): 396-407

[29] Hussein , A. K. ; Barrak, O. S. ; Hamzah , M. M. and Hussein S. Kh. (2025). Friction stir welding AA6061-T6 with multi-objective optimization of parameters. *Advances in Science and Technology Research Journal.* 19(10), 162–172. https://doi.org/10.12913/22998624/207049.

[30] Omar H. H., Mahmood M. H., Mursal L. S., Ghaith R. A., Azher S. B. and Yasir W. A. (2025). Thermal and Mechanical Analysis of Polyvinyl Chloride (PVC) to Polyethylene (PE) Bonding via Friction Stir Spot Welding Process. *Journal of Techniques*. 7 (2); 60-66. DOI: https://doi.org/10.51173/jt.v7i2.2686

[31] M. M. Hamzah1, S. M. Shnain, O. S. Barrak, S. Chatti, M. A. Al-Obaidi. (2025). Sustainable Friction Stir Spot Joining Process for Aluminum Alloy AA 4045 Parameter Optimization and Mechanical Assessment. *Annals of "Dunarea de Jos" University of Galati*. 36: 67-72. https://doi.org/10.35219/awet.2025.07 .